Supporting information

Twisted small organic molecules for high thermoelectric performance of single-walled carbon nanotubes/small organic molecule hybrids through mild charge transfer interactions

Yongjun Jeon[†a], Jae Gyu Jang[†a], Sung Hyun Kim[*b], and Jong-In Hong[*a]

[a] Department of Chemistry, Seoul National University, Seoul 08826, Republic of Korea; E-mail: jihong@snu.ac.kr.
[b] Department of Carbon Convergence Engineering, Wonkwang University, Iksan, Jeonbuk 54538, Republic of Korea; E-mail: shkim75@wku.ac.kr.
† These authors contributed equally.

Experimental

Materials

All chemicals were purchased from Alfa Aesar, Toyko Chemical Industry (TCI), and Samchun Co. Single-walled carbon nanotubes (SWCNTs, KH-SWCNT-HP) were purchased from KH chemicals (Korea).

Instruments

X-ray diffraction spectra of small organic molecules (SOMs), SWCNTs, and SWCNTs/ SOM were obtained using a SMART LAB (Rigaku) with a Cu Kα radiation. A field-emission scanning electron microscopy (FE-SEM, JEOL JSM-6701F) was performed to acquire the morphology data of SWCNTs and SWCNTs/SOMs films. Raman spectra of SWCNTs and SWCNTs/SOM were obtained using a Renishaw Invia Raman spectrometer with an Nd:YAG laser (λ = 532 nm). The charge carrier concentration and Hall mobility of SWCNTs and SWCNTs/SOM films were obtained using a Hall-effect measurement system (HMS-5000, Ecopia). Temperature-dependent resistance measurements for SWCNTs and SWCNTs/SOMs films were performed with a van der Pauw method with liquid nitrogen. Each SOM's HOMO and SWCNT's work function were obtained from photoelectron emission spectroscopy (Hitachi, High Tech AC-2)

Preparation of SWCNTs and SWCNTs/SOM films

SWCNTs powder (50 mg) was added into H_2O_2 (20 ml) solution and stirred at 334 K for 36 h. SWCNTs suspension was filtered through vacuum filtration apparatus, and the filtrate was washed with distilled H_2O (200 ml). SWCNTs solution was dispersed into tetrahydrofuran (THF, 100 ml) using a probe-type ultrasonicator (Bandelin HD 2070, MS 72 tip, 90 % power, cycles of 0.9 s on/0.1 s off) for 6 h in an ice water bath. A solution of SWCNTs/SOM was prepared by adding various weight percentages of SOMs into the SWCNTs (fixed amount) solution. Sequentially, the SWCNTs/SOM solution was mixed using a shaker (with 100 rpm) for 3 h. The glass substrate (20 × 20 × 7 mm) was washed with distilled H_2O and isopropyl alcohol (IPA) for 15 min in a bath-type sonicator (Branson 5510), respectively, and dried in a vacuum oven for 12 h. A solution (1 mL) of SWCNTs (or SWCNTs/SOM) was dropped onto the UV/ozone cleaned glass and annealed for 30 min at 393K. The washed SWCNTs/SOM films were prepared by dipping SWCNTs/SOM films into 20 ml dichloromethane (DCM) solution for 1, 3, 5, 10, 30, and 60 min, respectively. Then, the films were dried in air condition at 353 K for 1 h.

Preparation of organic thin films

A solution of 1.38 mg of each SOM (**TPE**, **TPA**, **TPE**+**TPA**, and **TPETPA**) dissolved in 1 ml of THF was dropped on the glass substrate (20 mm × 20 mm) which was heated to 120℃ and dried for 30 min. The glass substrates were prepared by the same procedure as in preparation of SWCNTs/SOM films.

Measurements of thermoelectric properties

The temperature differences of 2, 4, 6, and 8 K were induced to the films with two sheets of the Peltier device controlled by Keithley 2604B as the power source and the source meter. The temperature of the sample's surface was measured by a Keithley 2700 multimeter system. A Keithley 6485 picoammeter and a Keithley 2182A nanovoltmeter were utilized to measure the current and the potential difference between two electrodes on the sample.

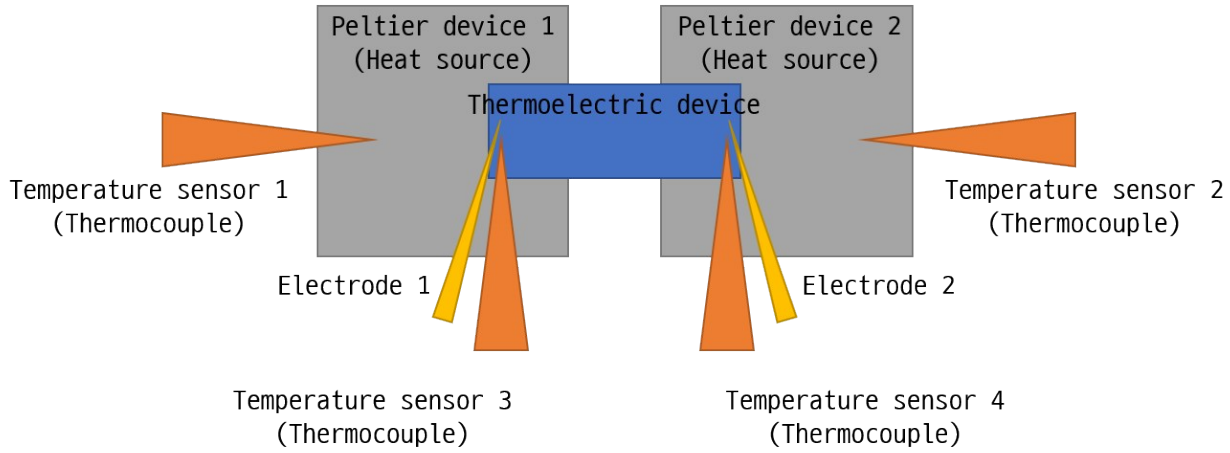

Scheme S1. Schematic illustration of the thermoelectric effect or thermoelectric generator performance measurement system

Temperature values are measured by temperature sensors 1-4 using a Keithley 2700 multimeter system. Electrodes 1-2 are connected to the internal switching system for the measurement of potential and current with Keithley 6485 and Keithley 2182A. Two sheets of Peltier devices are functioned as a heat source (temperature controller) and they are controlled by Keithley 2640B with the feedback signals from temperature sensors through Keithley 2700.

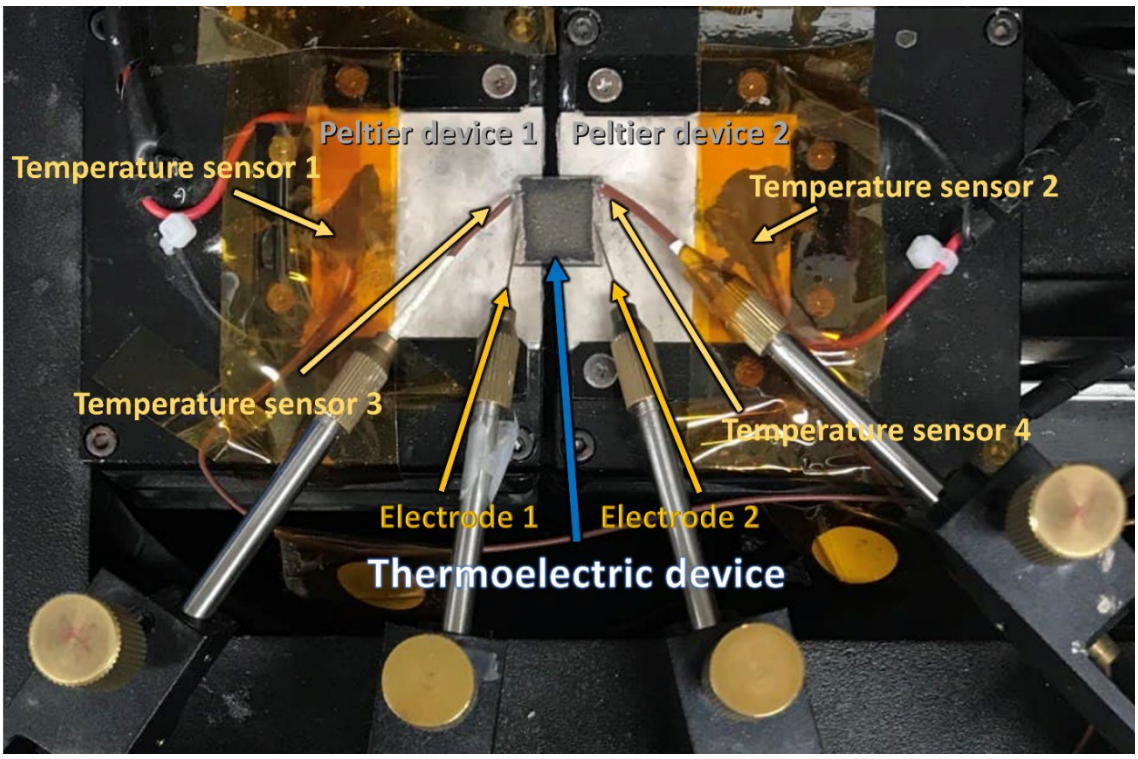

Scheme S2. Picture of the thermoelectric effect or thermoelectric generator performance measurement system.

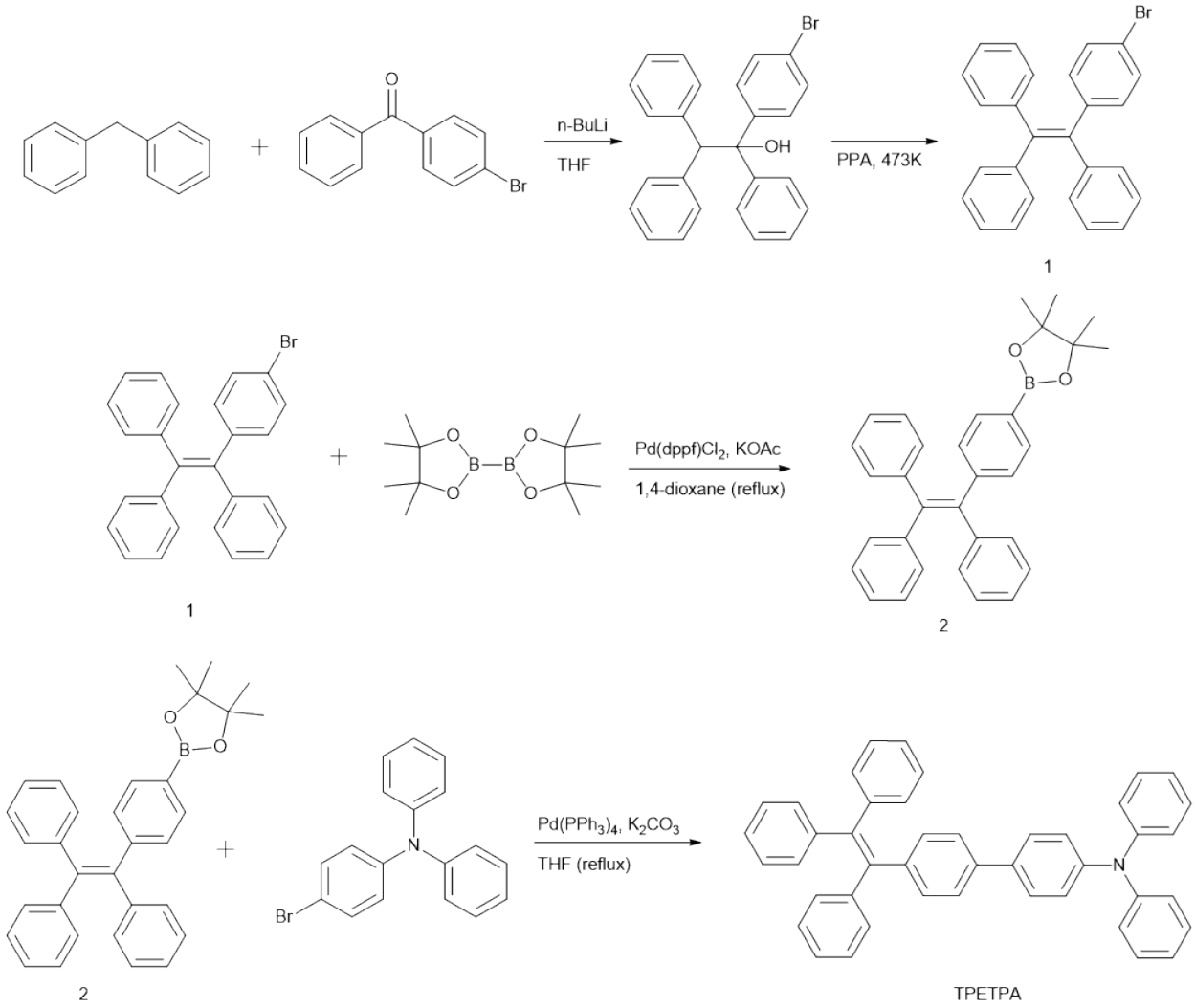

Scheme S3. Synthetic scheme of **TPETPA**.

Synthesis of TPETPA

Compound 1 To a solution of diphenylmethane (4.2 g, 25 mmol) in 100 ml of THF cooled to 0°C was added n-butyl lithium (22 mmol, 2.5 M in THF). After 30 min of stirring, 4-bromobenzophenone (5 g, 19 mmol) was added and the resulting mixture was stirred for 12 h. Then, crude (4-bromophenyl)-1,2,2-triphenylethan-1-ol (white powder, 6 g, 73%) was obtained by filtering. This crude product was added to 100 ml of polyphosphoric acid and heated at 200°C for 12 h. 100 ml of water was added to the reaction mixture and stirred 2 h. Finally, **1** was obtained by filtering. ^{1}H-NMR (300 MHz, acetone-d_6) 6.98 (d, J = 8 Hz, 2H), 7.05 -7.15 (m, 15H), 7.31 (d, J = 8 Hz, 2H).

Compound 2 A mixture of compound **1** (5.92 g, 14.4 mmol), bis(pinacolato)diboron (5.48g, 21.5 mmol), [1,1'-bis(diphenylphosphino)ferrocene]palladium(II) dichloride (1 g, 1.2 mmol), and potassium acetate (5.6 g, 57.6 mmol) dissolved in 100 ml of 1,4-dioxane was refluxed overnight. The reaction mixture was partitioned between water and dichloromethane. The organic layer was dried with anhydrous magnesium sulfate and filtered through Celite. Then the crude product was purified by column chromatography with hexane and ethyl acetate to furnish compound **2** (5.62 g, 84.8%). ^{1}H-NMR (400 MHz, $CDCl_3$) 1.53 (s, 12H), 6.95-7.04 (m, 8H), 7.04-7.10 (s, 9H), 7.52 (d, J = 8 Hz, 2H).

TPETPA A mixture of compound **2** (2.5 g, 5.4 mmol) and 4-bromotriphenylamine (1.4 g, 4.2 mmol), tetrakis(triphenylphosphine)palladium(0) (240 mg, 0.2 mmol), and potassium carbonate (3.5 g, 25 mmol) dissolved in 100 ml of THF and 30 ml of water was refluxed overnight. The reaction mixture was partitioned between water and dichloromethane. The organic layer was dried with anhydrous magnesium sulfate and filtered through Celite. Purification by column chromatography with hexane and ethyl acetate provided an orange solid (**TPETPA**, 1.4 g, 58%). ^{1}H-NMR (400 MHz, acetone-d_6) 7.00-7.15 (m, 25H), 7.28 (d, J = 4 Hz, 2H), 7.30 (d, J = 4 Hz, 2H), 7.42 (d, J = 8 Hz, 2H), 7.54 (d, J = 12 Hz, 2H).

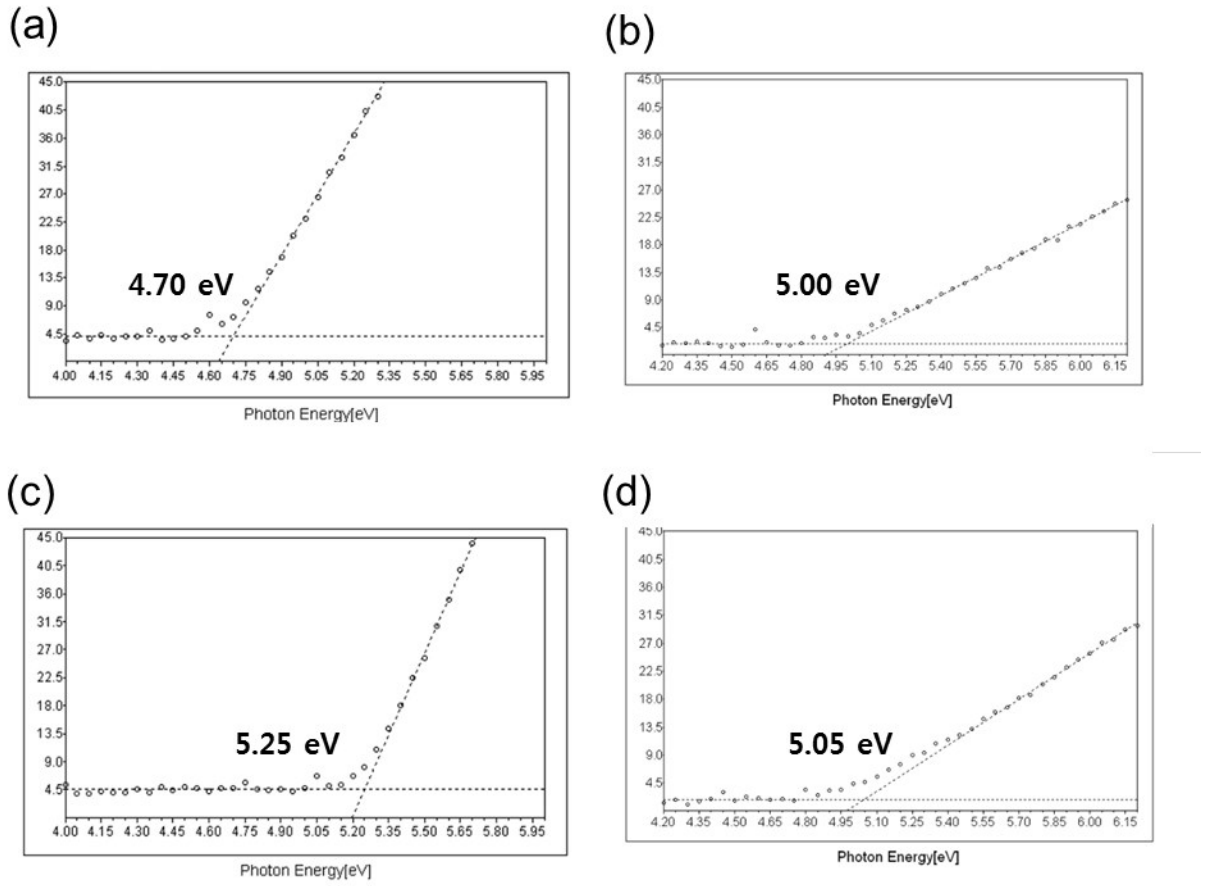

Fig. S1 (a) Valence band of SWCNTs (-4.70 eV), ionization energy levels of b) **TPE** (-5.00 eV), c) **TPA** (-5.25 eV), and d) **TPETPA** (-5.05 eV) films.

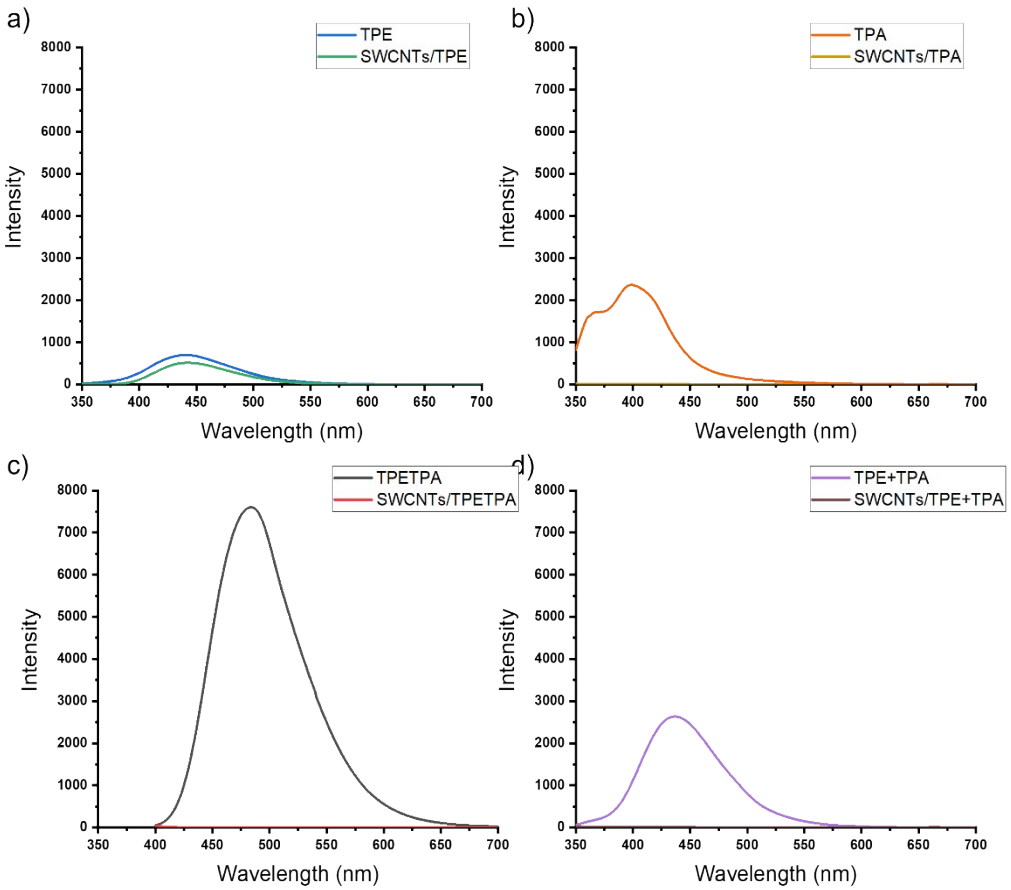

Fig. S2 The emission intensity of a) **TPE**, SWCNTs/**TPE**, b) **TPA**, SWCNTs/**TPA**, c) **TPETPA**, SWCNTs/**TPETPA**, and d) **TPE**+**TPA**, SWCNTs/**TPE**+**TPA** in thin film state. The blend ratio of SWCNTs/SOM is 13.8% (the mass fraction providing the maximum power factor). Excitation wavelengths are 385 nm for **TPETPA** and 332 nm for **TPA**, **TPA**, **TPE**+**TPA**.

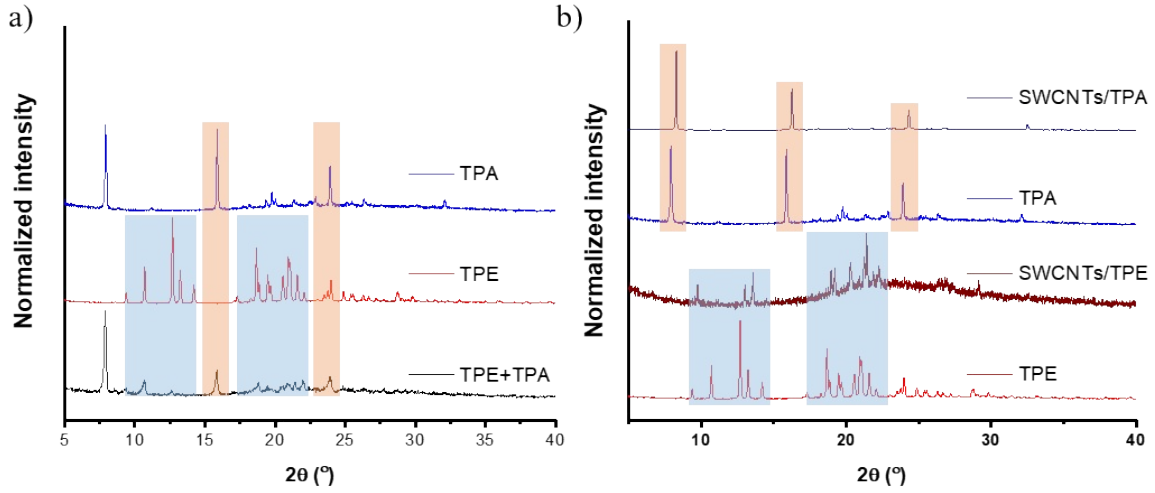

Fig. S3 Two sets of X-ray diffraction (XRD) spectra: a) XRD spectra of **TPA**, **TPE**, and **TPE**+**TPA** in film state, b) XRD spectra of SWCNTs/**TPA**, **TPA**, SWCNTs/**TPE**, and **TPE** in film state.

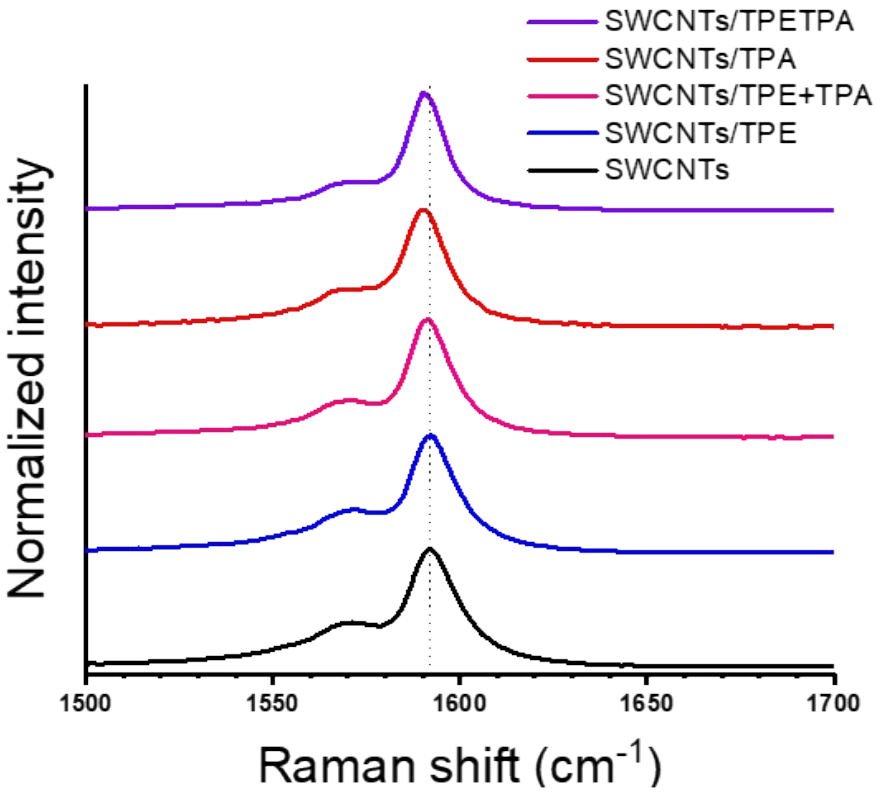

Fig. S4 Raman spectra of SWCNTs, SWCNTs/**TPE,** SWCNTs/**TPE**+**TPA**, SWCNTs/**TPA**, SWCNTs/**TPETPA**. G-bands of SWCNTs, SWCNTs/**TPE,** SWCNTs/**TPE**+**TPA**, SWCNTs/**TPA**, SWCNTs/**TPETPA** are 1592 cm^{-1}, 1592 cm^{-1}, 1591 cm^{-1}, 1590 cm^{-1}, and 1590 cm^{-1}, respectively.

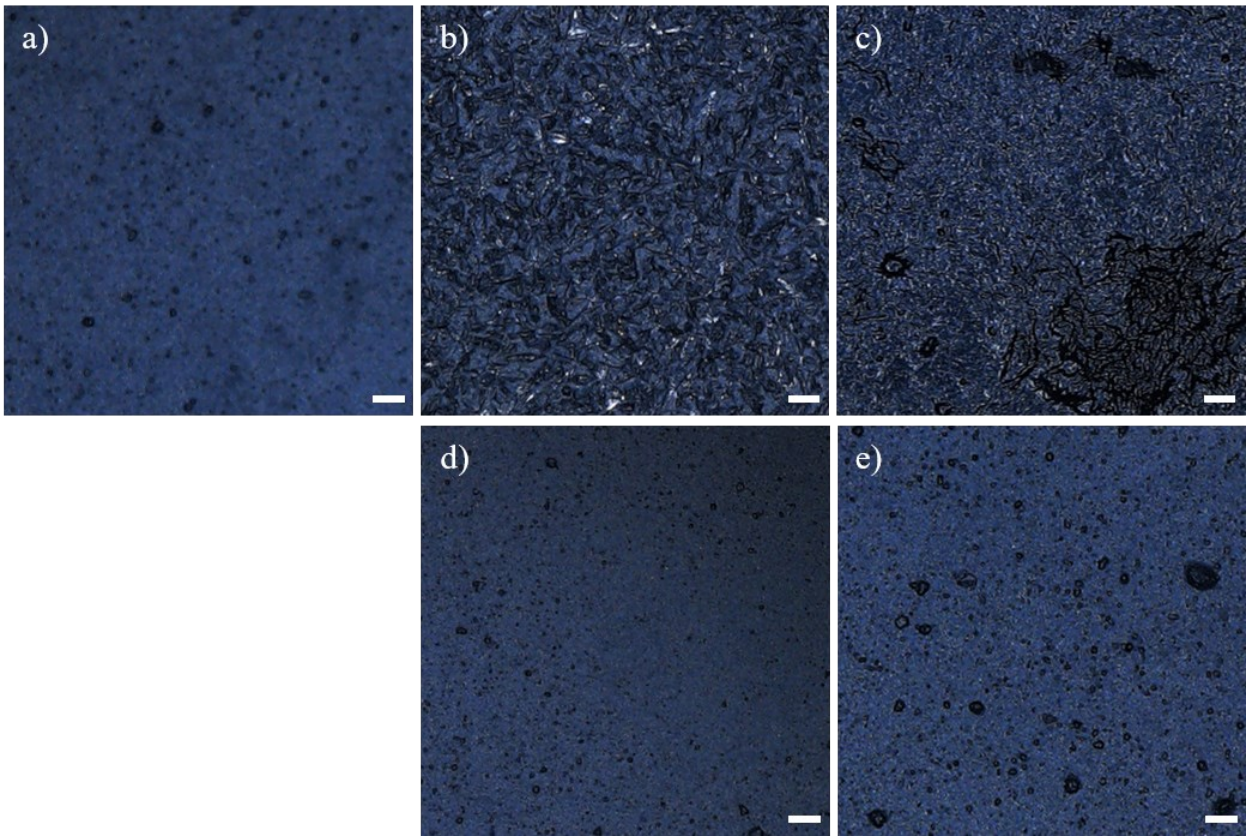

Fig. S5 Optical microscopic images of a) SWCNTs, b) SWCNTs/**TPE**, c) SWCNTs/**TPA**, d) SWCNTs/**TPE**+**TPA** and e) SWCNTs/**TPETPA**. The scale bar is 100 μm.

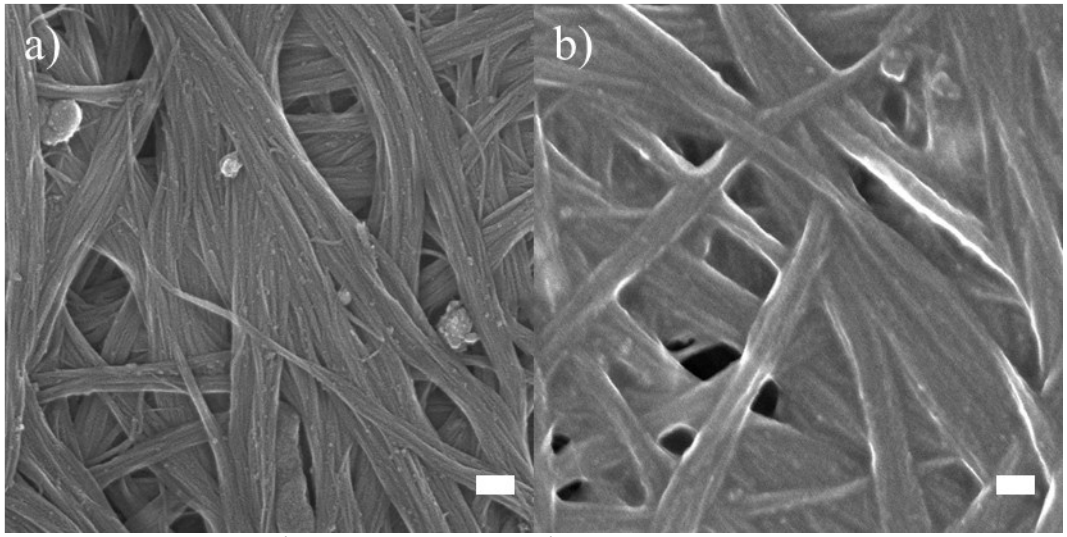

Fig. S6 FE-SEM images of (a) SWCNTs/**TPE**+**TPA** and (b) SWCNTs/**TPETPA** films. The scale bar is 100 nm. The mass fraction of **TPE**+**TPA** (or **TPETPA**) is 56.9 wt%.

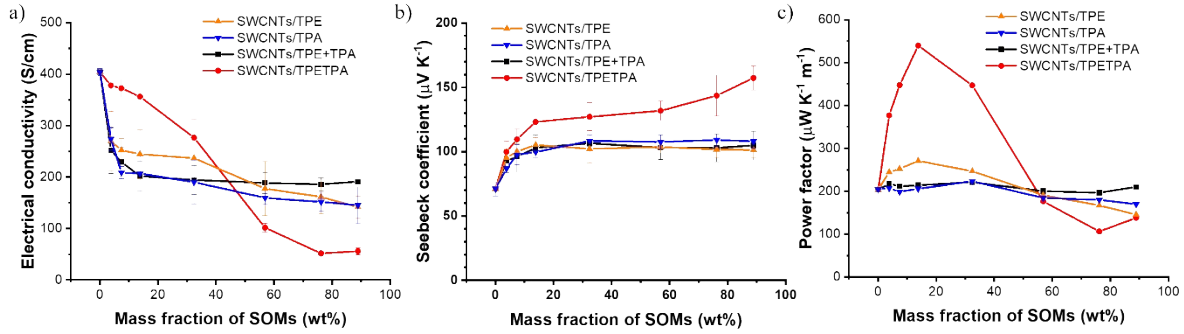

Fig. S7 TE properties of the SWCNTs/**TPE**, SWCNTs/**TPA**, SWCNTs/**TPE+TPA**, and SWCNTs/**TPETPA** films: (a) Electrical conductivity, (b) Seebeck coefficient, and (c) PF. The solid lines are eye visual guides.

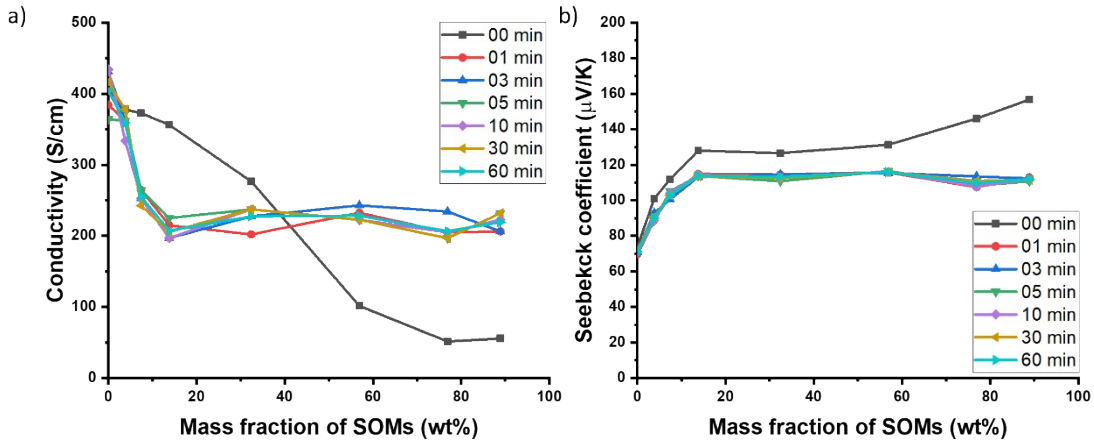

Fig. S8 TE properties of the pristine SWCNTs, and SWCNTs/**TPETPA** films as a function of mass fraction and different dipping time: (a) Electrical conductivities and (b) Seebeck coefficients of DCM-washed films.

Table S1. TE performance of previously reported p-type SWCNTs/SOMs hybrids

Sample	Electrical conductivity (S/cm)	Seebeck coefficient (μV/K)	Power factor (μW/m·K)	Reference
SWCNTs/ C_8C_{12}-NDI[a)]	515.6	55.49	158.8	1
TCNQ[c)] doped SWCNTs/C_8BTBT[b)]	885.4	56.6	284.6	2
SWCNTs/ZnTPPD[d)]	926.7	46.9	203.8	3
SWCNTs/TCzPy[e)]	189.4	75.9	108.4	4
SWCNTs/Por-5F[f)]	982.4	53.3	279.3	5
SWCNTs/ PhC_2Cu[g)]	666.2	55	200.2	6
SWCNTs/HAT6[h)]	1286.9	56.5	408.2	7

a) Naphthalenediimide with branched alkyl chain
b) 7,7,8,8-Tetracyanoquinodimethane
c) 2,7-Dioctyl[1]benzothieno[3,2-b][1]benzothiophene
d) Zinc Porphyrin
e) 1,3,6,8-tetrakis(3,6-di-tert-butyl-9H-carbazol-9-yl)pyrene
f) 5,10,15,20-Tetrakis(perfluorophenyl)porphyrin
g) Copper-phenylacetylide
h) 2,3,6,7,10,11-hexakis(hexyloxy)triphenylene

Table S2. In-plane thermal conductivity of SWCNTs and SWCNTs/organic molecule-based TE hybrids.

Sample	In-plane thermal conductivity (S/cm)	Reference
SWCNTs	20	8
SWCNTs	24	9
SWCNTs	35	10
SWCNTs/P3HT	0.43	11
SWNT/Flavin derivative	62.1	12
SWCNT/PEDOT:PSS	0.25	13

References

1 F. Liu, X. Zhou, C. Pan and L. Wang, *J. Power Sources*, 2019, **412**, 153-159.
2 J. Tan, Z. Chen, D. Wang, S. Qin, X. Xiao, D. Xie, D. Liu and L. Wang, *J. Mater. Chem. A*, 2019, **7**, 24982-24991.
3 Y. Zhou, Y. Liu, X. Zhou, Y. Gao, C. Gao and L. Wang, *J. Power Sources*, 2019, **423**, 152-158.
4 X. Yin, Y. Peng, J. Luo, X. Zhou, C. Gao, L. Wang and C. Yang, *J. Mater. Chem. A*, 2018, **6**, 8323-8330.
5 Y. Zhou, X. Yin, Y. Liu, X. Zhou, T. Wan, S. Wang, C. Gao and L. Wang, *ACS Sustain. Chem. Eng.*, 2019, **7**, 11832-11840.
6 N. Feng, C. Gao, C.-Y. Guo and G. Chen, *ACS Appl. Mater. Interfaces*, 2018, **10**, 5603-5608.
7 X. Li, Z. Yu, H. Zhou, F. Yang, F. Zhong, X. Mao, B. Li, H. Xin, C. Gao and L. Wang, *ACS Sustain. Chem. Eng.*, 2021, **9**, 1891-1898.
8 A. Duzynska, A. Taube, K. Korona, J. Judek and M. Zdrojek, *Appl. Phys. Lett.*, 2015, **106**, 183108.
9 T. Ma, Z. Liu, J. Wen, Y. Gao, X. Ren, H. Chen, C. Jin, X.-L. Ma, N. Xu and H.-M. Cheng, *Nat. Commun.*, 2017, **8**, 1-9.
10 J. Hone, M. Whitney, C. Piskoti and A. Zettl, *Phys. Rev. B*, 1999, **59**, R2514.
11 C. Bounioux, P. Díaz-Chao, M. Campoy-Quiles, M. S. Martín-González, A. R. Goni, R. Yerushalmi-Rozen and C. Müller, *Energy Environ. Sci.*, 2013, **6**, 918-925.
12 W. Huang, F. Toshimitsu, K. Ozono, M. Matsumoto, A. Borah, Y. Motoishi, K.-H. Park, J.-W. Jang and T. Fujigaya, *Chem. Commun.*, 2019, **55**, 2636-2639.
13 Q. Jiang, X. Lan, C. Liu, H. Shi, Z. Zhu, F. Zhao, J. Xu and F. Jiang, *Mater. Chem. Front.*, 2018, **2**, 679-685.